Earthquake Engineering, Tenth World Conference © 1992 Balkema, Rotterdam. ISBN 90 5410 060 5

Observation of earthquake strong-motion with deep borehole
Generation of vertical motion propagating in surface layers after *S* wave arrival

K.Takahashi, S.Ohno, M.Takemura & T.Ohta
Kajima Corporation, Tokyo, Japan

T.Hatori
Toda Corporation, Tokyo, Japan

Y.Sugawara
Tokyo Electric Power Company, Japan

S.Omote
University of Tokyo, Japan

ABSTRACT: Recently, in view of the new issues which have been raised concerning the vertical motion of floors and the security of valuable equipment installed in structures, the need for considering vertical earthquake motion has become more pronounced. In order to reveal the nature of the generation and propagation of vertical motion caused by earthquakes in surface layers, the authors conducted an examination of earthquake waveforms and particle motion orbits observed in base rock (granodiorite) and surface layers lying on the base rock. The observations were conducted in Tomioka, Japan. Simulation analyses were also performed. The results raise the possibility that the vertical components observed in the surface layers are mostly P waves converted from SV waves at the boundaries of the layers above the base rock.

1. INTRODUCTION

Before the design of a major structure is finalized, preliminary study on the dynamic aspects of the structure such as earthquake response analysis is often mandatory.

Horizontal motion has been emphasized in the earthquake response analysis of structures and in earthquake observations and analyses, because of the great effect it has on structures. Recently, however, in view of issues newly raised concerning the vertical motion of floors and the security of valuable equipment installed in structures, the necessity of considering vertical earthquake motion has increased.

Maximum acceleration, maximum velocity, and duration are frequently used for the evaluation of input design earthquake motion in earthquake response analyses. The frequency characteristics of earthquake ground motion are also taken into consideration in the design of high-rise buildings and facilities for nuclear reactors. The input design earthquake motion for structural design is generally given at the ground surface, or at the base of the structure, or in relatively shallow surface layers of the ground.

Research on the horizontal motion in surface layers of the ground has achieved progress and the results are reflected in the Japan Building Code and Regulatory guide for the aseismic design of nuclear power reactor facilities. Specifications on the characteristics of vertical motion in the above, however, are quite limited. One reason for this is that studies on vertical motion have lagged behind those on horizontal motion. The issues associated with vertical motion must be discussed based on the results of observations.

There have been relatively few studies on the characteristics of vertical motion in the surface layers. Attempts to grasp the nature of earthquake wave propagation through surface layers directly from the waveforms obtained by observations in vertical instrument arrays are particularly rare. Taking note of this situation, we conducted an examination of sesmic waveforms and particle motion orbits observed in base rock (granodiorite) and surface layers above base rock in Tomioka, Japan. Simulation analyses were also performed.

2. EARTHQUAKE OBSERVATION POINT AND UNDERGROUND STRUCTURE

The location of the Tomioka observation point (code name TMK), and the arrangement of the seismometers and underground structures are depicted in Figures 1 and 2.

The TMK observation point comprises six seismometering points in a vertical array of GL–950 m, GL–660 m, GL–251 m, GL–100 m, GL–6 m, and GL, together with two other seismometering points that combine with GL-6m to form a horizontal triangular array with sides about 150 m long.

The underground structure at TMK consists of base rock (granodiorite) below GL–815m and tertiary sedimentary rock lying on the base rock. Knowledge of the underground structure was obtained using PS logging and formation density logging by means of the deepest borehole (ref. 3).

3. EARTHQUAKE

The earthquake used in this paper occurred on June

26,1984. Its magnitude was 4.5 (JMA scale), the depth of hypocenter of 50 km, epicentral distance (Δ) of 55 km, and theoretical incident angle at the deepest seismometering point of 32° (see Figure 1). The theoretical incident angle was obtained by applying the epicentral distance and structure from Ichikawa and Mochizuki's travel time table (ref. 2).

4. EXAMINATION OF OBSERVATION RECORDS

4.1 *Waveforms*

The transverse (T) and radial (R) components were calculated by means of RT conversion of acceleration waveforms (NS, EW) in terms of the locations of seismometering points and the hypocenter. The velocity waveforms are obtained by integration.

These waveforms were pasted up in the direction perpendicular to the ground surface (downward). The acceleration waveform in Figure 3, the vertical component in P wave initial phase in Figure 4, and vertical and R components of S waves from initiation to major motion are shown in Figure 5.

The propagation times between seismometers of the waves moving upward, calculated from the results of PS logging, are shown in Table 1. In Figures 4 and 5, the onsets of P wave are adjusted to form solid lines if the wave propagates as described in Table 1. Elapsed time after the start of wave recording is plotted on the abscissas. The times of P and S wave arrival agreed roughly with those calculated using the travel time tables of Ichikawa and Mochizuki (ref. 2).

From Figures 3, 4, and 5, the followings can be pointed out:

(1) Importance of vertical component after S wave arrival

As shown in Figure 3, the amplitude of the vertical component after S wave arrival is generally greater than that before in surface layers, and the part after S wave arrival tends to persist longer. As structures are commonly built on surface layers, vertical motion after S wave arrival must be considered in aseismic design.

(2) Upward and downward travel of P waves during initial phase

In Figure 4, the onset of the vertical component is traveling from GL–950 m (base rock) to GL along straight line ① taking about 0.400 seconds. This time is less than the propagation time of the P waves with incident angle of zero, apparently because of propagation with some incident angle. Along solid line ② which is a symmetrical surface reflection of line ① the downward travel of the wave is apparent.

(3) Upward and downward travel of S waves during initial phase

As can be seen from solid lines Ⓑ and Ⓒ in Figure 5, the onset of the major motion of vertical component rises and falls just as in (2) at almost the same velocity as that of P waves. Therefore, it can be concluded from Figures 4 and 5 that vertical components in the initial phase of both P and S waves rise and fall equally at P wave velocity (V_P). In the case of straight line Ⓑ, the travel time of the component is about 0.37 seconds, approximately in agreement with the theoretical travel time calculated by the SV–P conversion assumption discussed below in (4).

On the other hand, the R component rises and falls in a manner as shown by broken lines D and E in Figure 5. The travel time of the R component is almost identical to the propagation time of S waves shown in Table 1, thus indicating that it rises and falls at the S wave velocity (V_S). The T component (not illustrated here) rises and falls at V_S just as the R component does.

(4) Conversion of SV waves to P waves

Because the phases of major motion of vertical and R components at GL–950 m are opposite from t=11.2 second and t=11.6 second, the waves arriving at this time are thought to be SV waves. The faulting duration time in earthquakes below magnitude 4.5 is estimated to be less than about 0.7 seconds (ref. 4), and it is likely that direct S waves are incident upon the base rock during the time section.

From GL–660 m upward the vertical component travels at V_P and the R component at V_S. However, V_S changes, to a great extent, in the section between GL–950 m and GL–660 m (surge impedance ratio: about 0.42), suggesting the occurrence of SV–P conversion at layer boundaries in this region.

Supposing that SV–P conversion takes place directly above the seismometering point at GL–950 m (▲ in Figure 5, t=11.20 second), the converted P wave arrives at GL at about t=11.57 (▼ in Figure 5) with the incident angle of SV waves taken into consideration. The arrival time of the direct S wave at GL is about t=12.14 (▽ in Figure 5). The dominance of the vertical component over the R component in the waveforms arriving at GL during the period between t=11.57 and t=12.14 supports the assumptions of SV-P conversion.

4.2 *Particle motion orbit*

Figure 6 and 7 show particle motion orbits at GL and GL-950 m, with maximum amplitudes (kine) for each time period noted atop them.

As may be seen in Figure 7, at GL–950 m the vertical component prevails over the horizontal components before S-wave arrival. In the initial phase of S waves the horizontal components are relatively dominant, and the particle motion orbits associated with SV waves reveals itself in the vertical-radial diagrams. A similar tendency are also seen at other instrument locations, and the ray paths of wave are observed to become more nearly vertical at shallower depths (not illustrated here).

Figure 6 shows that at GL, the vertical component is overwhelming between t=11.57 and t=12.14, which is presumed to be the interval between the arrival times of converted P waves and direct S waves. In other words, it is verified that SV-P converted waves arrive at GL before direct S wave arrival.

5. SIMULATION ANALYSIS

The authors attempted to explain analytically the results of the observations. The propagation of SV waves in a multi-layered soil deposits with some incident angle given below were calculated using the method of Haskell, 1958 (ref. 1).

The damping factors used in the response analyses were determined by evaluating the data collected by field tests and laboratory tests of boring cores. The values of the constant are 0.03 for the section between GL and GL–4.8 m, 0.02 between GL–4.8 and GL–470 m, and 0.01 below GL–470 m.

5.1 *Travel time*

Figure 8 shows the responses at each seismometering point in the case that 100 Hz Ricker wavelet is SV incident wave at GL–950 m waves. The incident angle was assumed to be 30°. This response analysis is intended to confirm the travel times of SV and P waves. In Figure 8, R and vertical components are represented by broken and solid lines, respectively. In line Ⓐ the occurrence of SV–P conversion at GL–660 m is obvious and this part is dominanted by the vertical component. The travel time from GL–950 to GL is 0.370 seconds, which is distinctly short compared with the 0.406 seconds in the case of incident P wave at an incident angle of 0° and 0.396 seconds at an incident angle of 30°, and is consistent with the results attained in the examination of waveform observations.

5.2 *Response analyses*

Earthquake response analyses were performed on the assumption that the vertical component observed at GL–950 m was that of SV waves and that the R component observed was the horizontal component of SV waves. Figures 9 and 10 show the results of the analyses, together with the results of observations for comparison. These figures indicate that the results of the observations can be explained well not only in the section before S arrival but also in the section after S arrival, if the observed waveforms at GL-950 m are SV waves with some incident anlgle.

From the foregoing, it can be said that the vertical component observed in the surface layers is considered as P waves, which are produced by SV–P conversion at the boundaries of the layers above the base rock.

6. CONCLUSION

The possibility has been revealed by the examination of observation records and simulation analyses that the vertical components observed in surface layers after S wave arrival in the base rock are mostly P waves converted from SV waves during their ascent from the base rock.

Seismic waveform with a vertical instruments array at Tomioka prove that the vertical component of initial phase of S waves travels up and down at the same velocity as that of P waves in the surface layers above the base rock. The waveforms and particle motion orbits indicate that the occurrence of SV–P conversion in the section between GL–950 m and GL–660 m are thought to be the cause of this phenomenon.

We also examined six other earthquakes of minor magnitude ($M \fallingdotseq 4.0$ to 4.5, $\Delta = 42$ to 74 km). The results of investigation of them concur with the result of this paper with unquestionable clarity.

Therefore, regarding vertical motion observed in and on the ground, sufficient consideration must be paid to the fact that the vertical motion which is attributed to the motion of S waves can be characterized by P waves.

Further, the nature of vertical motion abovementioned must be sufficiently considered in the treatment of input earthquake motion in earthquake response analyses for aseismic design.

Finally, we conclude this report with an additional statement that conclusions identical to those described above have been obtained by examining the results of earthquake records at the Iwaki observation point, which, like TMK, is a vertical instruments array that stretches from base rock to ground surface (GL–330 m to GL) (ref. 3, 5).

ACKNOWLEDGEMENTS

Valuable earthquake data were offered by "Committee of Strong-Motion Instruments Array" sponsored by ten electric power companies in Japan, which is very much appreciated.

REFERENCES

1. Haskell, N. A. 1953. The dispersion of surface waves on multilayered media., Bull. Seismol. Soc. Am., 43, 17-34.
2. Ichikawa, M., E.Mochizuki 1971. Travel Time Tables for Local Earthquakes In and Neaar Japan, Papers in Meteorology and Geophysics Vol. 22, 229-290. (in Japanese with English abstract)
3. Omote, S, Y.Ohsawa, B.Ohmura S.Iizuka, T.Ohta and K.Takahashi, 1984. Ohservation of Earthquake Strong-Motion with Deep Boreholes -An Introductory Note for Iwake and Tomioka Observation Station in Japan -, 8WCEE.
4. Sato.R. 1979. THEORETICAL BASIS ON RELATIONSHIPS BETWEEN FOCAL PARAMETERS AND EARTHQUAKE MAGNITUDE, J.Phys. Earth, 27, 353-372.
5. Takahashi, K., S.Omote, T.Ohta, T.Ikeura and S.Noda 1988. OBSERVATION OF EARTHQUAKE STRONG-MOTION WITH DEEP BOREHOLE - COMPARISON OF SEISMIC MOTIONS IN THE BASE ROCK AND THOSE ON THE ROCK OUTCROP - , 9WCEE.

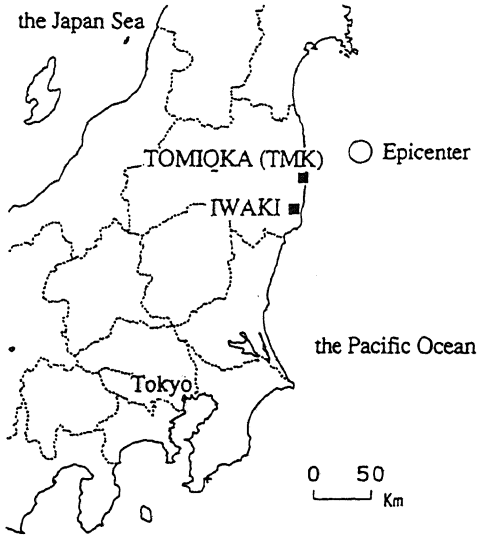

Fig. 1 Location of Observation Station and Epicenter

Table 1 Travel time between seismometers (second)

Observation Level	Travel time calculated from underground structure	
	S wave	P wave
GL		
- 100m	0.207	0.066
- 251m	0.178	0.075
- 660m	0.390	0.179
- 950m	0.179	0.086
	——	——
Total	0.954	0.406

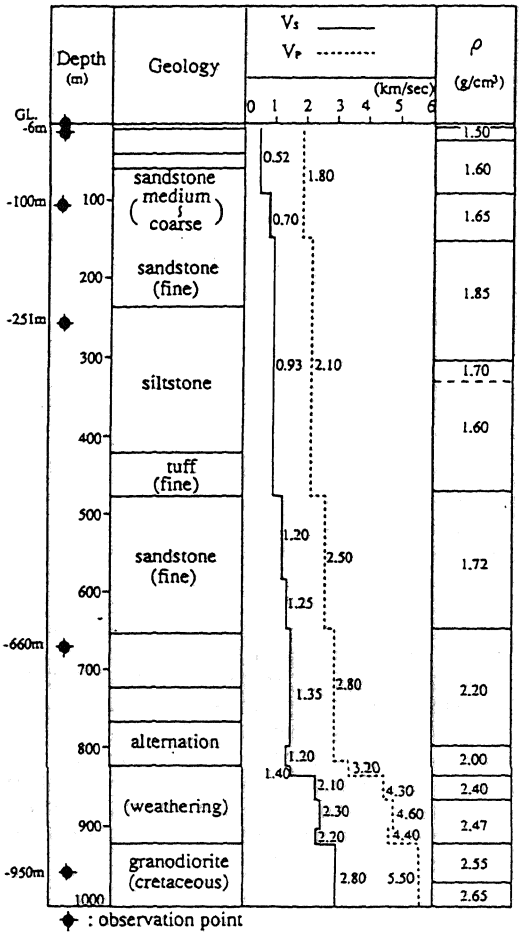

Fig. 2 Geological Structure and Station level at TMK

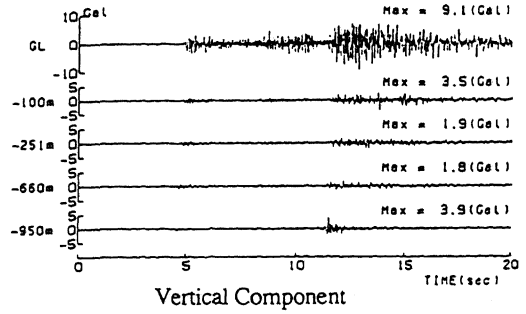

Vertical Component

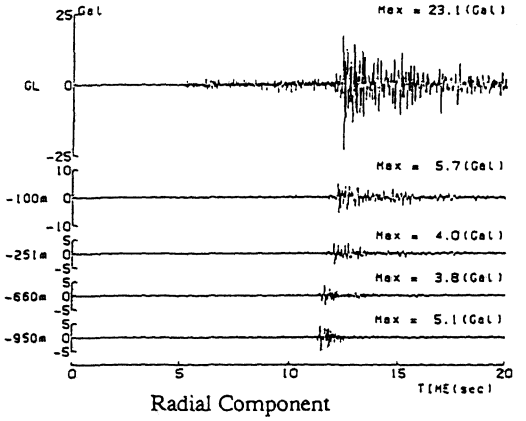

Radial Component

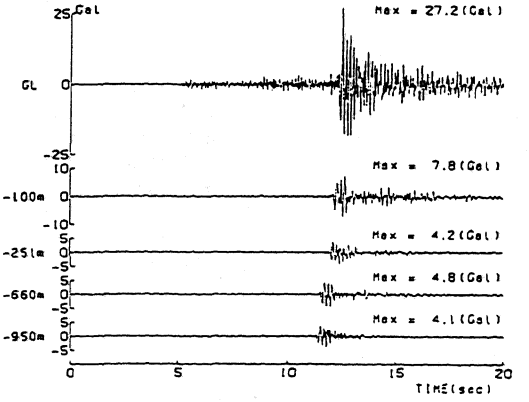

Transeverse Component

Fig. 3 Seismograms from TMK (Acceleration)

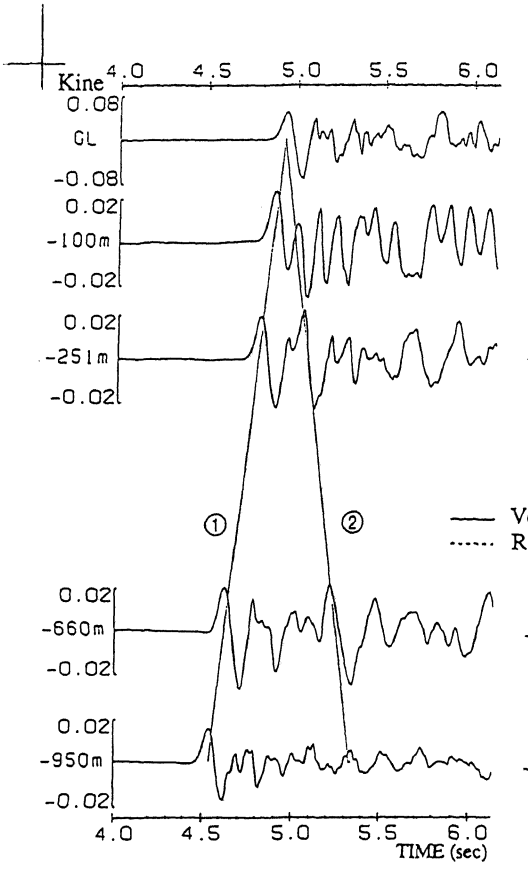

Fig. 4 Close-Up of Initial Motions of Seismograms in Fig.3 (Vertical Component, Velocity)

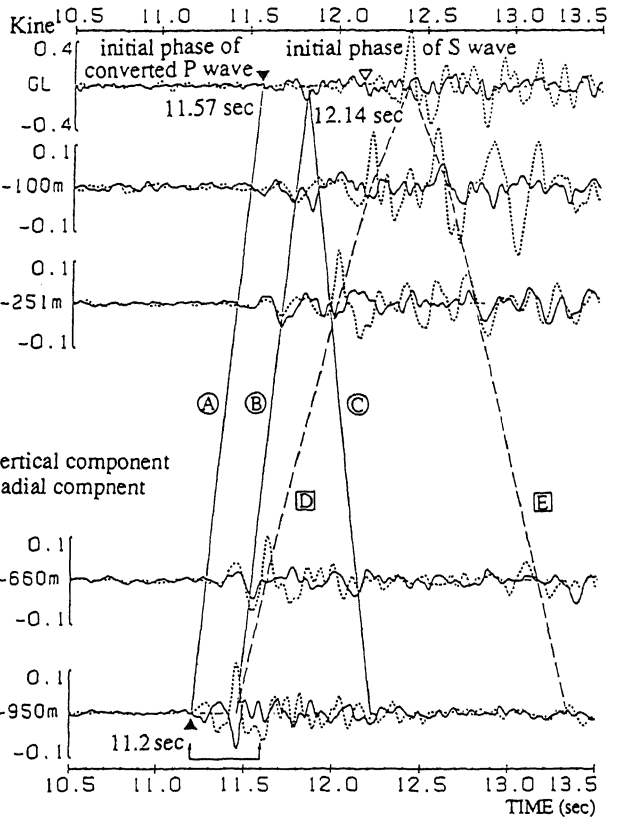

Fig. 5 Close-Up of Part of S-wave of Seismograms in Fig.3 (Vertical Component and Radial Component., Velocity)

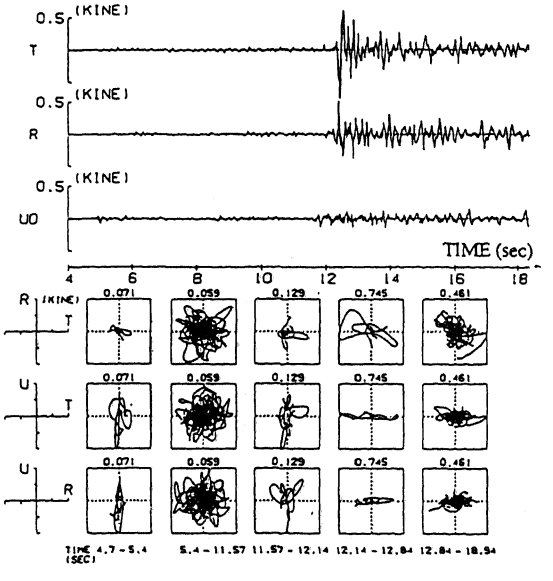

Fig. 6 Particle Motion Orbits at GL

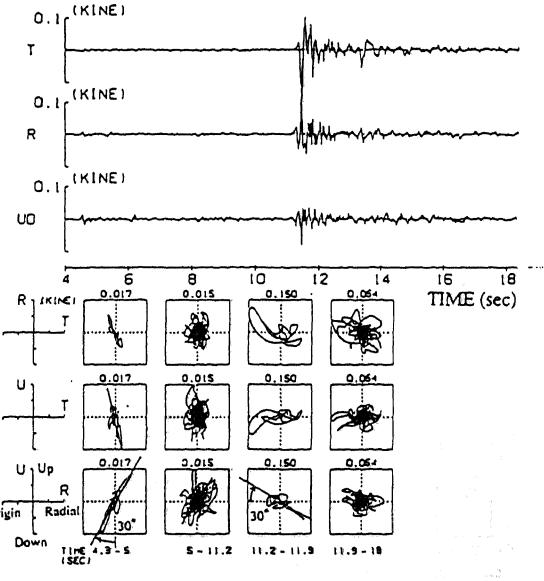

Fig. 7 Particle Motion Orbits at GL-950 m

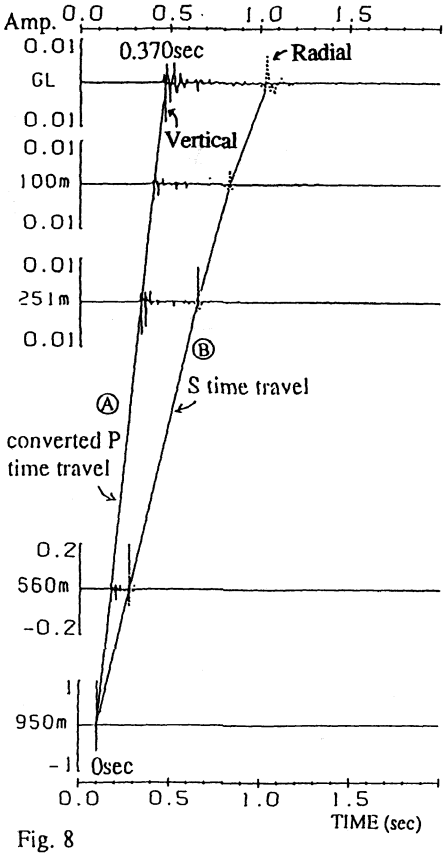

Fig. 8
Calculated waveforms when 100 Hz Ricker wavelet arrived at GL-950 m for incident SV waves with incident angle of 30 degrees

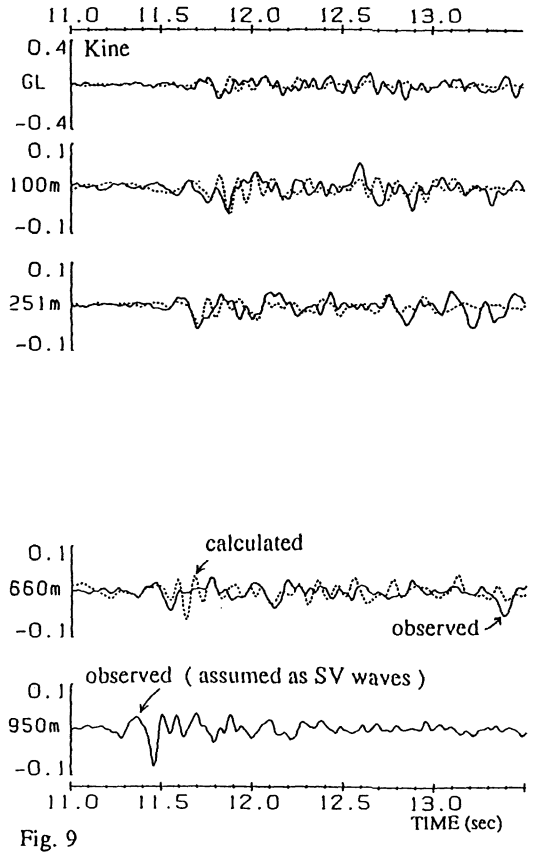

Fig. 9
Comparison vertical components waveforms between observed and calculated for incident SV waves

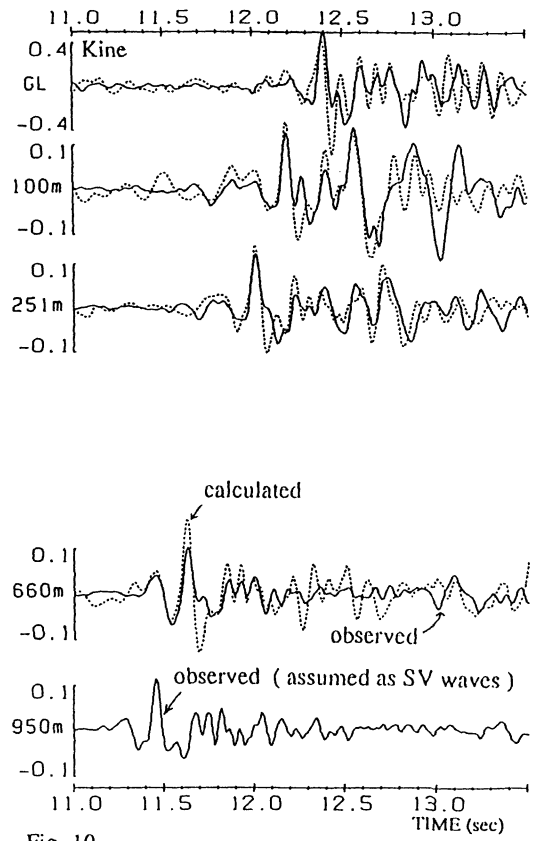

Fig. 10
Comparison radial components waveforms between observed and calculated for incident SV waves